doi:10.1038/nature10588

Observed increase in local cooling effect of deforestation at higher latitudes

FLUXNET and surface station data

Data obtained at 33 FLUXNET eddy flux forest sites are used in this analysis (Figure S1, Table S1). These sites have a minimum of 3 years of continuous temperature and net radiation data. One surface weather station is chosen in the closest proximity to every forest site for the paired analysis. The elevation difference of the 33 site pairs has a mean value of 59 m and shows statistically insignificant correlation with latitude (linear correlation = 0.006, n = 33). The average linear distance is 28 km and the average latitudinal distance is 0.2 km. The two site pairs with the largest distances (91 and 70 km) are in Canada's prairie provinces (Saskatchewan and Manitoba, respectively); these separations are mostly longitudinal, with latitudinal differences of 1 and 13 km, respectively. Small corrections are made for the elevation difference using site-specific lapse rates derived from the NARR dataset.

NARR data

NARR is a high-frequency, high resolution data assimilation model for North America[25]. It uses the NCEP Eta model and numerous data sources to produce outputs at a grid spacing of 32 km. Surface station observations of the screen-height temperature are not used to constrain the modeled fields; rather this temperature is predicted using the Monin-Obukhov similarity function from the temperature at the lowest model grid, typically 10-80 m above the surface.

Each forest site is matched up with the closest NARR grid. The temperature observations at the forest and its paired surface station are then compared with the NARR screen-height temperature. A small lapse rate correction is applied to the NARR temperature if the grid surface elevation is different from that of the forest or the surface station. Figure 4 shows a comparison of the annual mean DTR among the three data sources. Similar to Figure 1a, Figure S2 shows that the annual temperature difference (station - NARR) becomes more negative with increasing latitude.

Uncertainties of the temperature comparisons

One source of uncertainty is related to the mismatch in the height of temperature measurements. All atmospheric models (GCMs, numerical weather forecast models, and reanalysis models including NARR) produce a surface air temperature for the standard model screen height of 2.0 m above the vegetation, which matches closely with the WMO-specified screen height of 1.5 m for surface air temperature observations. So it is appropriate to standardize the comparisons at this height. The height of the temperature measurement in the FLUXNET network varies from 2 to 15 m above the canopy. According to the data from a subset of the forest sites where measurements were made at multiple heights, the annual mean temperature is not sensitive to measurement height. On average, the annual temperature gradient is -0.0054 ± 0.0117 K m^{-1} (mean ± 1SD of four forest sites) in the surface layer above the treetops. The insensitivity to measurement height is a consequence of strong mixing which is a universal character of turbulent flow above forests. Scaling the FLUXNET measurements to the standard screen height would change the annual mean temperature by no more than 0.1 K. The annual mean DTR is slightly more sensitive to height, with a gradient of -0.042 ± 0.005 K m^{-1}. Correcting the FLUXNET data to the screen height would increase the DTR by 0 to 0.6 K. This correction can only explain 0-20% of the observed DTR difference between the forests and the surface stations.

A second source of uncertainty lies in the relationship between the surface-layer air temperature $T_{s,a}$ and surface temperature T_s. Surface temperature is not measured by the station network and is available only for small number of FLUXNET sites and over much shorter durations than for $T_{s,a}$. We have extended the insights gained through the surface energy balance analysis to interpreting the biophysical effect on the surface air temperature. Although the observed $T_{s,a}$ differences (Figures 1 - 2) are robust features independent of the energy balance analysis, it is nevertheless useful to quantify how well the observed $T_{s,a}$ approximates T_s. At the FLUXNET grassland and clear-cut sites, the annual $T_{s,a}$ appears slightly higher than T_s, with a mean $T_{s,a} - T_s$ of 0.37 K and SD of 0.59 K (n = 8). A nearly identical difference is found for the forest sites where the T_s measurement is available ($T_{s,a} - T_s = 0.30 \pm 0.61$ K, n = 16). Neither of the $T_{s,a} - T_s$ datasets shows dependence on latitude. The large standard deviations are mostly a consequence of deriving T_s from the surface longwave radiation measurement which has an uncertainty of 5-10 W m^{-2}. That

$T_{s,a}$ has similar warm biases for the forests and the open lands suggests that the observed latitudinal dependence (Figure 1) should also hold for T_s.

Formulation of the intrinsic biophysical mechanism

The intrinsic biophysical mechanism consists of several factors. In a hypothetical situation where energy transfer involves only radiation processes and atmospheric feedbacks are absent, the energy balance equation is given by

$$S + L_{\downarrow} - \sigma T_s^4 = 0 \quad \text{(S1)}$$

where the net shortwave radiation is given by $S = (1-a)K_{\downarrow}$, a is surface albedo, $K_{\downarrow}$ is solar radiation flux incident on the surface, $L_{\downarrow}$ is incoming longwave radiation, σ is the Stephan-Boltzmann constant, and T_s is surface temperature. If the net shortwave radiation is changed by ΔS, the outgoing longwave radiation will adjust accordingly, in a process termed the longwave radiation feedback[30], and the surface temperature will change to $T_s + \Delta T$ to establish a new state of energy balance

$$S + \Delta S + L_{\downarrow} - \sigma(T_s + \Delta T_s)^4 = 0 \quad \text{(S2)}$$

Manipulating Equations (S1) and (S2) yields the solution for ΔT_s

$$\Delta T_s = \lambda_0 \Delta S \quad \text{(S3)}$$

where $\lambda_0 = 1/(4\sigma T_s^3)$, the temperature sensitivity resulting from the longwave radiation feedback, is a weak function of T_s, varying from 0.22 to 0.16 K/(W m^{-2}) over the temperature range 270 – 300 K. This sensitivity is lower than the global value of 0.3 K/(W m^{-2}) (ref[30]).

In the real atmosphere, the actual temperature change is also dependent on energy redistribution through convection and evaporation in the atmospheric boundary layer (ABL), and the proper framework for this is the complete surface energy balance equation

$$S + L_{\downarrow} - \sigma T_s^4 = H + LE + G \quad \text{(S4)}$$

where H is sensible heat flux, LE is latent heat flux, and G is heat storage in the soil and the biomass. Here H and LE are given as

$$H = \rho C_p \frac{T_s - T_a}{r_a} \quad \text{(S5)}$$

$$LE = \frac{H}{\beta} \tag{S6}$$

where ρ is air density, C_p is specific heat of air at constant pressure, T_a is air temperature at the blending height z_b in the ABL, r_a is aerodynamic resistance and β is Bowen ratio. Linearizing the surface longwave radiation term in Equation (S4) and making use of Equations (S5) and (S6), we obtain a solution for T_s from Equation (S4):

$$T_s - T_a = \frac{\lambda_o}{1+f}(R_n^* - G) \tag{S7}$$

where R_n^* is an apparent net radiation given by

$$R_n^* = S + L_\downarrow - \sigma T_a^4 \tag{S8}$$

and the energy redistribution factor f is given by

$$f = \frac{\rho C_p}{4 r_a \sigma T_s^3}(1 + \frac{1}{\beta}) \tag{S9}$$

Let us now consider in the vicinity of one another a forest and an open land that share the same background climate state: they receive the same amounts of incoming shortwave radiation $K_\downarrow$ and incoming longwave radiation $L_\downarrow$ and air is sufficiently blended at height z_b[27] so that T_a is identical between the two locations. The net shortwave radiation is $S + \Delta S$ and S in the open land and in the forest, respectively. Differentiating Equation (S7) and ignoring minor terms such as surface emissivity changes and changes in G[7,31], we obtain Equation (1) in the main text, which is reproduced here for the reader's convenience

$$\Delta T_s \approx \frac{\lambda_0}{1+f}\Delta S + \frac{-\lambda_0}{(1+f)^2} R_n \Delta f \tag{S10}$$

This derivation also recognizes that $\Delta R_n^* = \Delta S$ and $R_n^* \approx R_n$ ($= S + L_\downarrow - \sigma T_s^4$).

The change in the energy redistribution factor Δf in Equation (S10) is given by

$$\Delta f = \Delta f_1 + \Delta f_2 \tag{S11}$$

$$\Delta f_1 = -\frac{\rho C_p}{4\sigma T_s^3 r_a}(1 + \frac{1}{\beta})\frac{\Delta r_a}{r_a} \tag{S12}$$

$$\Delta f_2 = -\frac{\rho C_p}{4\sigma T_s^3 r_a}\left(\frac{\Delta\beta}{\beta^2}\right) \quad \text{(S13)}$$

So the expanded form of Equation (S10) is given as

$$\Delta T_s \approx \frac{\lambda_0}{1+f}\Delta S + \frac{-\lambda_0}{(1+f)^2} R_n \Delta f_1 + \frac{-\lambda_0}{(1+f)^2} R_n \Delta f_2 \quad \text{(S14)}$$

The first, second and third term on the right side of Equation (S14) represent radiative forcing associated with albedo change, energy redistribution associated with roughness change and energy redistribution associated with Bowen ratio change, respectively.

A number of points regarding the above conceptual formulation merit the reader's attention. (**i**) A distinction is made between external forcing and internal feedback. Changes in the net shortwave radiation are a forcing term external to the system. On the other hand, changes in the surface longwave radiation are treated as an internal feedback mechanism, not part of a radiative forcing, in a manner consistent with the formulation of the global climate sensitivity[30]; (**ii**) Energy redistribution is also an internal process, but unlike feedbacks in the global system where they amplify the climate sensitivity, here it always damps the sensitivity. This explains why the observed local climate sensitivity [0.012 to 0.027 K/(W m^{-2})] is much lower than the sensitivity of the global climate system which is estimated at ~0.8 K/(W m^{-2}) (ref[32]); (**iii**) In the deforestation scenario, Δf_1 is primarily caused by the change in surface roughness (z_o), and is negative because r_a is proportional to $(1/u_*)\ln(z_b/z_o)$ and the friction velocity u_* is scaled by z_o according to the Rossby similarity relationship[33]. (**iv**) Traditionally, decreases in canopy conductance and soil moisture (and therefore surface evapotranspiration) are thought to increase the surface temperature. Equation (S14) shows that ΔT_s actually responds to changes in β or in how the radiation energy is partitioned; decreases in LE alone do not necessarily lead to a higher surface temperature. In Equation (S14), $\Delta\beta$ can be either negative or positive in response to deforestation. The inverse relation to β^2 (Equation S13) means that $\Delta\beta$ has a large contribution to ΔT_s in the tropical climate where β is small (e.g., $\beta = 0.3$, ref[14]; Figure 3e-f) and a negligible contribution in the semi-arid climate (e.g., $\beta = 6.6$, ref[34]; Figure 3d). (**v**) One way to further improve our understanding of the biophysical mechanism is to quantify how the energy distribution factor f varies among the major biomes of the world. Toward that end, f can be

backed out from measurements of all the other terms in Equation (S7), thus avoiding the more difficult determination of r_a and β in Equation (S9).

The energy balance model of the intrinsic biophysical mechanism is used in two ways to support the interpretation of the experimental data. First, inference is made from the model that changes in the surface temperature should become larger in magnitude at higher latitudes (see the main text). Second, the model is used in a conceptual factor separation analysis to unravel how various biophysical forcings reinforce and counteract one another. Equation (S14) is applied to six FLUXNET site clusters (Table S2) to partition the surface temperature change into contributions by radiative forcing, energy redistribution associated with changes in surface roughness and energy redistribution associated with changes in Bowen ratio. The calculation is done separately for the daytime and nighttime periods to avoid nonlinear parameter interactions through the diurnal cycle (Figures S3 & S4). In the main text, the results are presented as 24 h mean values (Figure 3). In this calculation, site-specific values are used for λ_0 , r_a is calculated according to the formulation of ref[35], and β is determined with the measured fluxes of H and LE.

Diurnal asymmetry of the biophysical effect

An important conclusion of this study is that the biophysical effect is not symmetrical through the course of the day. We have proposed two mechanisms for the asymmetry and have used the factor separation model to unravel how these mechanisms counteract one another. The first mechanism is related to changes in the net shortwave radiation and is relatively straightforward. According to Equations (S14), the impact of the radiative forcing term occurs in the daytime and vanishes at night. For example, at the FLUXNET site cluster in Saskatchewan (cluster *a*, Table S2), the radiative forcing of deforestation is predicted to cause a mean annual daytime cooling of about 2 K (Figure S3a) and no change in the nighttime temperature (Figure S4a). (The predicted 24 h mean temperature change associated with the radiative forcing is about -1 K, Figure 3a.)

The second mechanism concerns energy redistribution near the ground. In the daytime, open lands, being aerodynamically smoother, are less efficient than forests in dissipating heat into the ABL via turbulent diffusion, and as a result warm up faster than forests[34]. This "convector effect"[6] operates in the opposite direction of the radiative forcing and can even outweigh the

latter (Figure S3). At night in stably stratified conditions, on the other hand, open lands cool faster than forests (Figure 2c). We hypothesize that forests are warmer at night than open lands because the presence of trees causes turbulence which brings heat from aloft to the surface. The same process takes place in orchards at night when wind machines are used to promote turbulence in order to reduce the risk of frost[36]. Additional evidence for this hypothesis comes from two lines of reasoning. First, friction velocity (u_*) is higher in forested lands than in the adjacent open lands. For example, the annual mean nighttime u_* is 0.30 and 0.16 m s^{-1} at the jack pine forests and the harvested site, respectively, of the FLUXNET site cluster *a* (Table S2). Similarity arguments suggest that the downward heat transport from the atmosphere to the surface should be proportional to u_*^2 (ref[37]); Second, the second term of Equation (S14) is negative at night, implying more downward heat transfer over forests than over open lands. (The reader is reminded that $R_n < 0$ and $\Delta f_1 < 0$ in the deforestation scenario.) The FLUXNET cluster data show that at the mid- to high latitudes, the energy redistribution associated with the roughness change contributes about 0.5 K to the net cooling of the open lands relative to the forests at night (Figure S4 a-d).

Omitted in our analysis are possible changes in the heat storage term G in response to deforestation. This omission is justified for the daily mean temperature change because G is negligible when averaged over periods of 24 h and longer. However, the daytime and nighttime G may respond differently to deforestation. At the FLUXNET site cluster *a*, the only one that has measurements of biomass as well as soil heat storage, ΔG is slightly positive in the day, indicating that more solar energy is stored in the soil and biomass in the harvested site than in the jack pine forests (Table S3). It appears that in these forests, heat storage in the standing biomass is not enough to compensate for the reduction in soil heat storage caused by shading. At night, ΔG is slightly negative, indicating that more heat is released to the air from the soil and biomass in the harvested site than in the jack pine forests. The change in G is an external forcing on the surface climate whose contribution to the surface temperature change can be dealt with in the same manner as with ΔS

$$\Delta T_s = \frac{-\lambda_0}{1+f}\Delta G \qquad \text{(S15)}$$

(cf Equation S7). The calculations with Equation (S15) suggest that changes in *G* should reduce rather than enhance the diurnal temperature range (DTR) of the harvested land in comparison to that of the forests (Table S3). That the observed DTR is higher at the harvested site (12.7K) than at the forests (10.2K) indicates that changes in *G* are unlikely to be a factor contributing to the diurnal asymmetry of the biophysical effect.

The diurnal asymmetry is important for the assessment of the land use effect. If only the daily maximum temperature data were used, open land would be 0.42 ± 0.44 K and 1.28 ± 1.14 K warmer than forested land north and south of 45^{o}N, respectively, which is an erroneous result.

References

30 National Research Council, *Understanding Climate Change Feedbacks* (The National Academies Press, 2003).

31 Gu, L. et al. Influences of biomass heat and biochemical energy storages on the land surface fluxes and radiative temperature. *J. Geophys. Res*. **112**, D02107 (2007).

31 IPCC, Summary for Policymakers (SPM), in *Climate Change 2007: The Physical Science Basis: Contribution of Working Group I to the Fourth Assessment Report of the Intergovernmental Panel on Climate Change*, S. Solomon *et al.*, Eds., Cambridge Univ. Press, New York (2007).

33 Garratt, J. R. *The Atmospheric Boundary Layer*, 316 pp., Cambridge Univ. Press, New York (1992).

34 Rotenberg, E. & Yakir, D. Distinct patterns of changes in surface energy budget associated with forestation in the semi-arid region, *Global Change Biol*. 1**7**, 1536 (2011).

35 Stewart, J. B., et al., Sensible heat flux-radiometric surface temperature relationship for eight semiarid areas, *J. Appl. Meteorol*., **33**, 1110 (1994).

36 Ribeiro, A. C., et al. Apple orchard frost protection with wind machine operation. *Agric. Forest Meteorol*., **141**, 71 (2006).

37 Massman, W. J. & Lee, X. Eddy covariance flux corrections and uncertainties in long-term studies of carbon and energy exchanges. *Agric. Forest Meteorol*., **113**, 121 (2002).

Table S1: FLUXNET forest sites used for the paired analysis (weather station versus forest)

Site ID	Location	PI(s)
Bartlett	New Hampshire	A Richardson
BC_88	British Columbia	A Black
Black Spruce Cut	Quebec	H Margolis
Blodgett	California	A Goldstein
Borden	Ontario	R Staebler
Donaldson	Florida	T Martin
Duke Hardwood	North Carolina	G Katul / R Oren
Duke Pine	North Carolina	G Katul / R Oren
Eastern Old Black Spruce	Quebec	H Margolis
Flagstaff Unmanaged	Arizona	T Kolb
Great Mountain	Connecticut	X Lee
Harvard Forest	Massachusetts	W Munger / S Wofsy
Howland	Maine	D Hollinger
Kennedy Oak	Florida	B Drake
Lost Creek	Wisconsin	P Bolstad / K Davis
Metolius First	Oregon	B Law
Metolius Inter	Oregon	B Law
Metolius Old	Oregon	B Law
Missouri Ozark	Missouri	L Gu / S Pallardy / T Meyers
Mize	Florida	T Martin
MMSF	Indiana	H Schmid
Niwot Ridge	Colorado	R Monson
Northern Old Black Spruce	Manitoba	W Munger / S Wofsy
Old Aspen	Saskatchewan	A Barr
Old Black Spruce	Saskatchewan	A Barr
Old Jack Pine	Saskatchewan	A Barr
UCI_1850	Manitoba	M Goulden
UCI_1930	Manitoba	M Goulden
UCI_1981	Manitoba	M Goulden
UCI_1989	Manitoba	M Goulden
UMBS	Michigan	P Curtis
Walker Branch	Tennessee	T Meyers
Wind River	Washington	K T Paw U

Table S2: FLUXNET site clusters used for the conceptual factor separation analysis. Data for clusters *a*-*d* and *f* are obtained from public data archives (AmeriFlux, Fluxnet-Canada and LBA) and include air temperature, radiation balance, sensible and latent heat fluxes and friction velocity. Data for cluster *e* include surface temperature, air temperature, net radiation and heat fluxes found in ref[14] and friction velocity data provided by the site investigator.

Cluster	Climate	Forest(s)	Open land	Location	Reference(s)
a	Boreal	Jack pines	Harvested	Saskatchewan, Canada	17
b	Boreal	Black spruces	Burnt	Manitoba, Canada	18
c	Temperate	Oak – hickory, Loblolly pine	Grass	North Carolina, USA	19
d	Semi-arid	Pinyon juniper	Open shrub	California, USA	20
e	Tropical	Rainforest	Pasture	Rondônia, Brazil	14
f	Tropical	Rainforest	Farmland	Pará, Brazil	21,22

Table S3: Changes in the soil and biomass heat storage ΔG (open land – forest) and in the surface temperature ΔT_s predicted according to Equation (S15). The observations were made in the boreal FLUXNET site cluster in Saskatchewan (cluster *a*, Table S2). The data are presented as site-year mean value and one standard deviation of variations.

Time period	ΔG (W m^{-2})	ΔT_s (K)
Daytime	4.5 ± 4.3	-0.18 ± 0.17
Nighttime	-3.1 ± 3.5	0.32 ± 0.35

Figure S1: Map of the FLUXNET forest sites used for the paired analysis (weather station versus forest)

Figure S2: Difference in the screen-height temperature between the NARR prediction and the station observation as a function of latitude. Parameter bounds in the linear regression are for the 95% confidence level

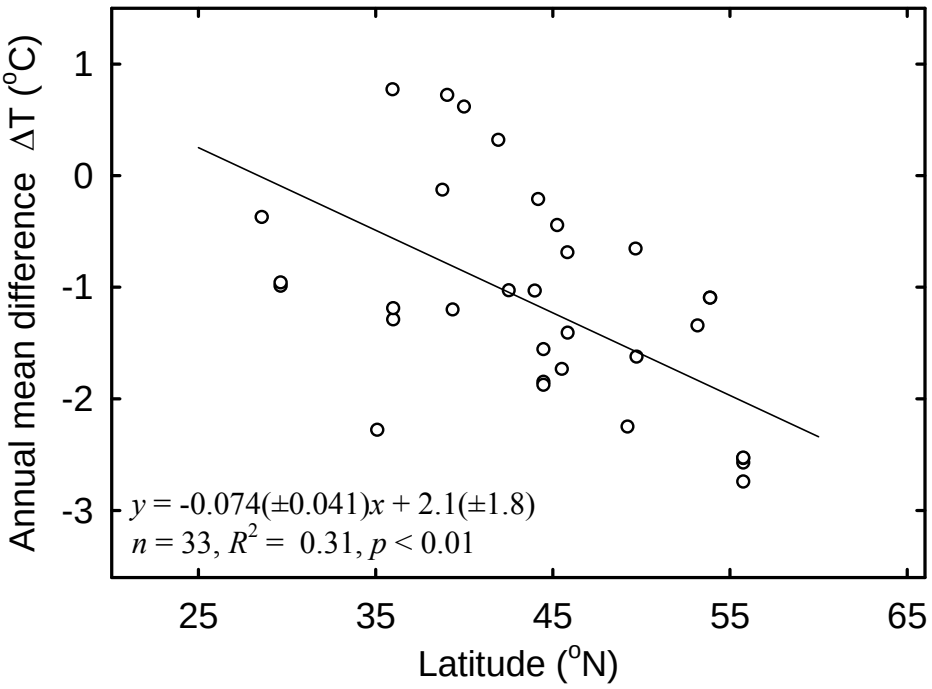

Figure S3: Partition of the *daytime* biophysical effect at the six FLUXNET site clusters shown in Table S2. Error bars are given as 1SD for the clusters with multiple site-year observations. No surface temperature measurements are available for clusters b and d, and no temperature data are available to compute daytime and nighttime means for cluster e. For comparison, observed changes in surface air temperature (ΔT) are also shown

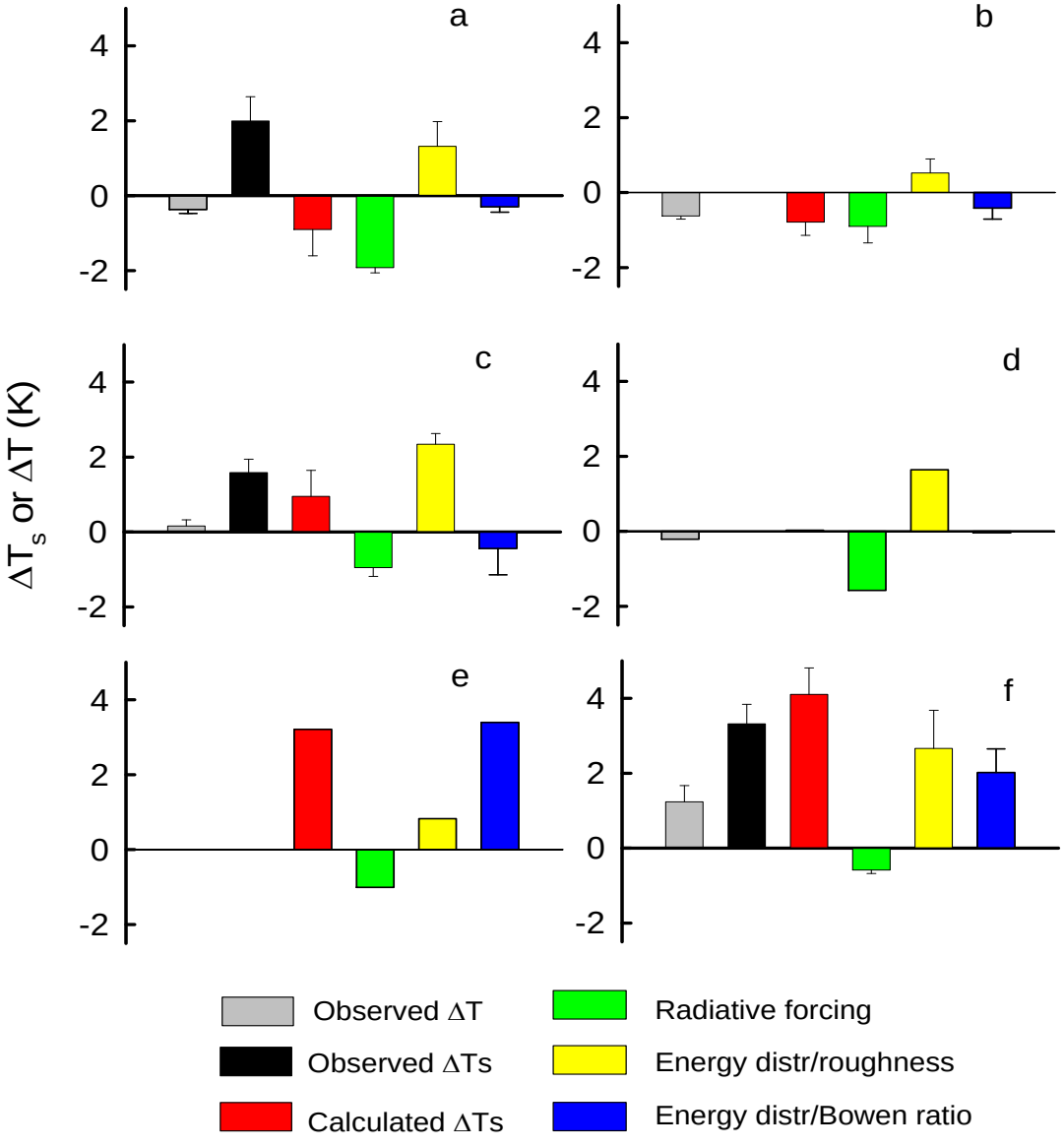

Figure S4: As in Figure S3 except for nighttime